Observation of band gaps in the gigahertz range and deaf bands in a hypersonic aluminum nitride phononic crystal slab

M. Gorisse,[1,a)] S. Benchabane,[2] G. Teissier,[1] C. Billard,[1] A. Reinhardt,[1] V. Laude,[2] E. Defaÿ,[1] and M. Aïd[1]
[1]*CEA, Leti, MINATEC Campus, 17 rue des Martyrs, 38054 GRENOBLE Cedex 9, France*
[2]*Institut FEMTO-ST, CNRS, Université de Franche–Comté, 32 Avenue de l'Observatoire, 25044 Besançon Cedex, France*

(Received 26 April 2011; accepted 18 May 2011; published online 10 June 2011)

We report on the observation of elastic waves propagating in a two-dimensional phononic crystal composed of air holes drilled in an aluminum nitride membrane. The theoretical band structure indicates the existence of an acoustic band gap centered around 800 MHz with a relative bandwidth of 6.5% that is confirmed by gigahertz optical images of the surface displacement. Further electrical measurements and computation of the transmission reveal a much wider attenuation band that is explained by the deaf character of certain bands resulting from the orthogonality of their polarization with that of the source. © *2011 American Institute of Physics*. [doi:10.1063/1.3598425]

Phononic crystals[1,2] (PCs) are periodical structures composed of two or more materials. As their optical counterparts, photonic crystals, they support frequency band gaps where propagation of elastic waves is prohibited. Microscale PCs have attracted a lot of attention recently, due to their potential applications to filters, waveguides and vibration insulators in radio-frequency devices and microelectromechanical systems. Following shortly the demonstrations of PCs for surface acoustic waves,[3–5] a great interest has arisen for PCs for Lamb waves in PC slabs.[6–10] Experimental demonstrations have been made with two dimensional arrays of holes in silicon[6,7] or in aluminum nitride[8] membranes, or in arrays made of tungsten inclusions embedded in a silicon dioxide matrix.[9,10]

The demonstration of the existence of band gaps is most often conducted via electrical measurements. On a membrane, such electrical measurements require an emitting and a receiving Lamb wave transducers, e.g., implemented as sets of interdigitated metal electrodes.[11,12] Frequency band gaps are revealed by comparing the electrical transmission between emitter and receiver for a reference device and for the PC. As pointed out by Soliman *et al.*,[10] such an analysis suffers from an experimental bias since band gaps are measured indirectly via transducers that do not exhibit a frequency independent transfer function. Optically imaging the propagation of elastic waves in a PC has been demonstrated for surface acoustic waves.[13] In addition to clear pictures of wave propagation and diffraction by the PC, such optical measurements provide one with knowledge of the polarization of the waves, at least with regards to the surface displacements.

In this letter, we study experimentally the propagation of guided waves in a two dimensional PC composed of air holes drilled in an aluminum nitride membrane. Combining gigahertz (GHz) optical and electrical measurements and comparing with computations of the transmission and the polarization of Bloch waves in the PC, we find an attenuation band much larger than the phononic band gap as a result of the existence of many deaf bands.

The PC we designed is composed of a square array of holes drilled in a free standing aluminum nitride (AlN)/silicon dioxide (SiO_2) membrane. The lattice parameter is $a=6.6$ μm and the radius of the inclusions is $r=2$ μm, hence resulting in a filling fraction of about $f=0.29$. The thickness of the membrane is $h=2$ μm for the AlN layer and 500 nm for the SiO_2 layer underneath. We designed a delay line composed of an emitting interdigitated transducer (IDT), a transmission area with the PC, and a receiving transducer identical to the emitting one, as shown in Fig. 1. The PC is fabricated using a three masks process.[12] Silicon dioxide (SiO_2) is thermally grown on a high resistivity Si wafer. Molybdenum electrodes are then deposited by sputtering and patterned by reactive ion etching using fluorine chemistry. The piezoelectric aluminum nitride (AlN) layer is then deposited by pulsed-dc reactive sputtering. Top electrodes (Al) are sputter-deposited and patterned. AlN and SiO_2 are dry etched through a SiO_2 mineral mask. Finally the membrane is released by chemically etching Si using XeF_2 gas. At this stage, the bottom silicon dioxide film is used to protect the bottom molybdenum electrodes from being chemically etched during the release step. The overall process is fully complementary metal-oxide semiconductor-compatible and is realized on 8 in. wafers.

Electrical measurements were performed on wafer using a vector network analyzer and coplanar rf probes. rf measurements were performed between 10 MHz and 5 GHz,

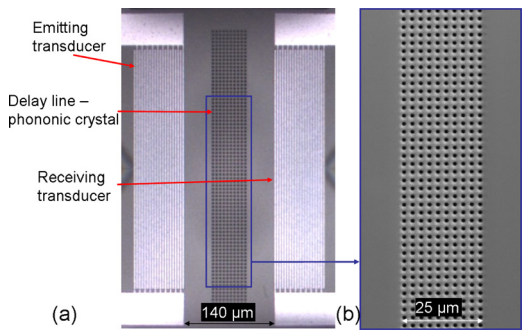

FIG. 1. (Color online) (a) Optical photograph of the PC delay line and (b) scanning electron micrograph of the PC region.

[a)]Electronic mail: marie.gorisse@cea.fr.

 © 2011 American Institute of Physics

Author complimentary copy. Redistribution subject to AIP license or copyright, see http://apl.aip.org/apl/copyright.jsp

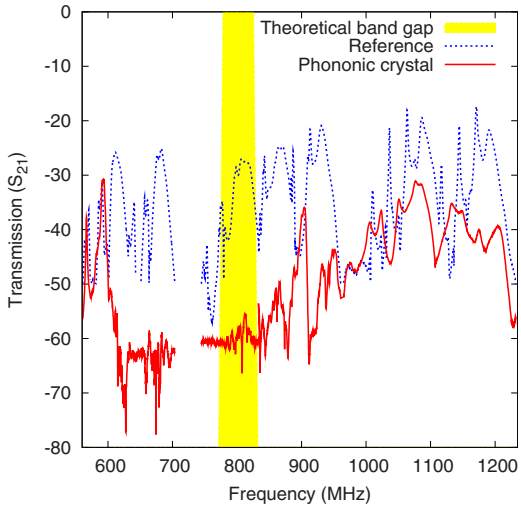

FIG. 2. (Color online) Electrical measurement of the transmission of guided elastic waves with (solid curve) and without the phononic crystal (dashed curve).

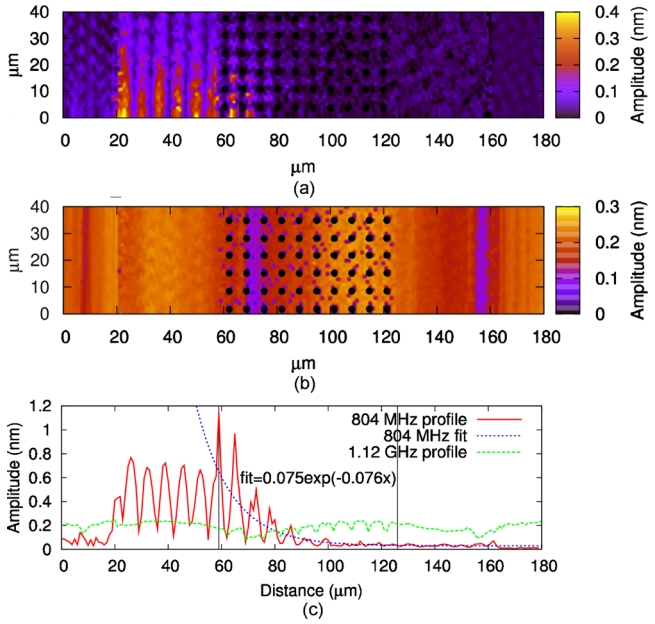

FIG. 3. (Color online) Optical measurement of the transmission trough a PC at (a) 804 MHz and (b) 1120 MHz. (c) Profile of the amplitude in and above the band gap integrated along y and fit of the attenuation in the PC.

with more accurate frequency steps of 200 kHz between 100 MHz to 2 GHz to optimize the measurement accuracy in this band. A full two-port Short-Open-Load-Thru calibration was done. A semiautomatic rf prober was used to ensure repeatable contact resistance between the different devices.

Electrical transmission curves are shown in Fig. 2 for reference devices and devices including the PC. To cover the 550 MHz–1.2 GHz frequency band, a set of six devices were measured, due to the limited bandwidth of each IDT. The theoretical band gap extends from 776 MHz to 828 MHz and is indicated by the band on Fig. 2. The electrical measurements show an attenuation of the transmission between 600 and 900 MHz, much larger than the expected band gap, as was recently observed.[10] A possible explanation is that the incident waves emitted by the source may not be able to couple into all modes of the PC.[14] We can still see relatively good transmission below 600 MHz and above 950 MHz, even with regard to the decrease in the signal level that is due to reflection of elastic waves at the entrance and at the exit of the PC.

Optical imaging of the amplitude of out of plane vibrations resulting from the application of a single frequency rf signal onto the emission transducer only was next conducted using a heterodyne laser probe similar to the one described in Ref. 15, here, only allowing amplitude detection. An area of 180 μm $\times$ 40 μm hosting the PC was scanned with a lateral scanning step of 1 μm in both directions. Results are shown in Fig. 3. The measurement at 804 MHz, inside the theoretical band gap, reveals a standing wave between the emitting IDTs and the PC caused by reflection of the Lamb wave propagating in the AlN/SiO_2 membrane at the PC entrance. The wave is then attenuated inside the PC, the wave amplitude on the other side of the PC structure being almost zero. The profile of the amplitude is plotted in Fig. 3(c). An exponential fit provides an attenuation of about 0.53 Np per wavelength. The second measurement, above the theoretical band gap (at 1120 MHz) shows propagation through the PC with low attenuation.

Propagation in the PC was modeled using the finite element method (FEM). The band structure was obtained by applying Bloch periodic conditions at the edges of a unit-cell of the PC, hence modeling a perfect infinite PC.[16] The obtained band structure is presented in Figs. 4(a) and 4(b) and shows a directional phononic band gap extending between 776 MHz and 828 MHz along the ΓX direction. This gap is relatively narrow (6% relative frequency width) due to the low filling fraction (0.29) chosen for ease of fabrication. We further computed the acoustic transmission using FEM. We forced an arbitrary displacement closely reproducing the polarization of the Lamb wave excited by the emitting IDT (S_0 mode) at the edge of a supercell composed of a row of 10 elementary cells of the PC, and performed a harmonic simulation. Perfectly matched layers were added at the edges of the computation domain to absorb outgoing waves without causing noticeable reflection. The theoretical acoustic transmission is presented in Fig. 4(c) along with the measured electrical transmission. The measured transmission is calculated by subtracting the reference signal to the PC signal, which causes the positive transmission. A rather good agreement between experiment and theory is observed. In particular, the occurrence of a wide attenuation band extending between 600 and 900 MHz is confirmed by the computed transmission.

In order to explain the difference between the band gap expected from the band diagram and the attenuation band observed in the transmission spectrum, we point at the polarization of waves guided in the membrane. First, the incident S_0 Lamb wave with elliptical polarization in the sagittal plane cannot couple into all Bloch modes of the PC. Second, mode conversions occurring at the boundaries of the PC may excite not only the S_0 mode, but also the A_0 and SH_0 modes which are little or not piezoelectrically coupled, and are thus "electrically invisible." In addition the SH_0 mode, with ideally no vertical displacement cannot be detected by laser interferometry and thus should not appear in the optical scans shown in Fig. 3.

We plot in Fig. 4(a) the band structure with indication of the dominant polarization for each Bloch mode. This dominant polarization represents the direction of the largest dis-

Author complimentary copy. Redistribution subject to AIP license or copyright, see http://apl.aip.org/apl/copyright.jsp

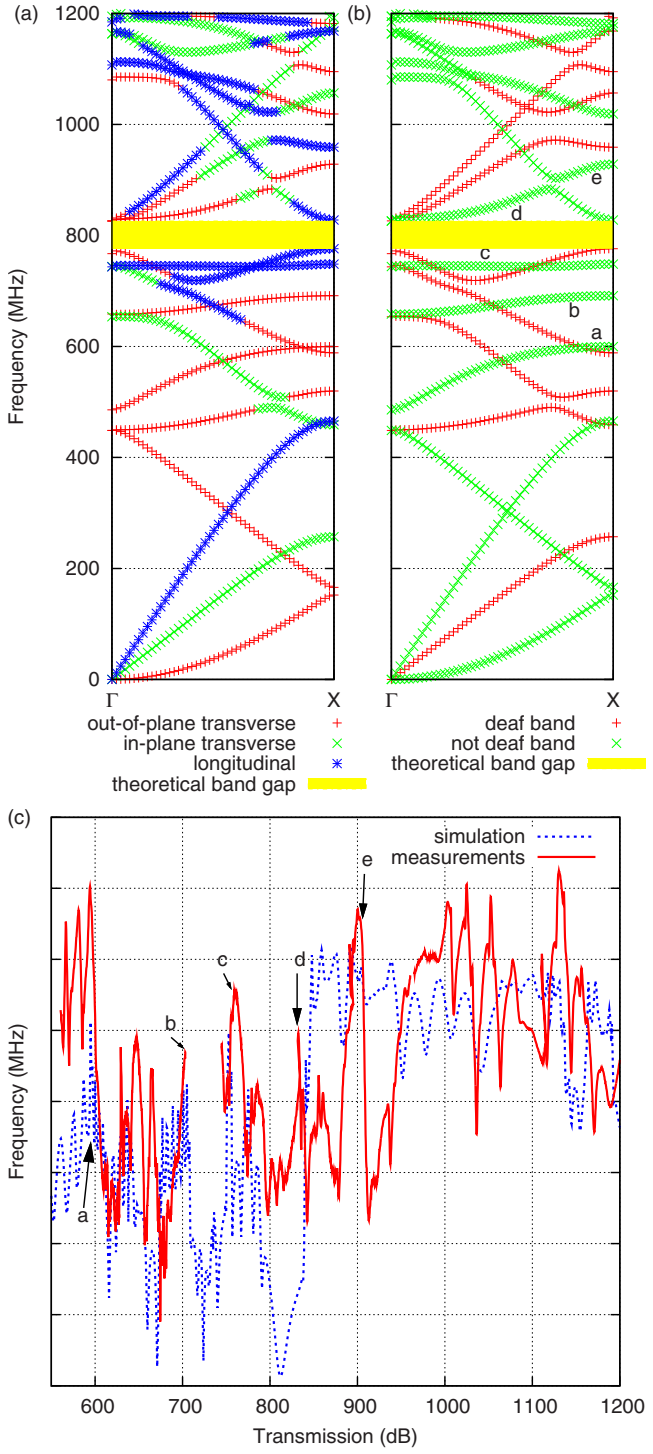

FIG. 4. (Color online) Band structure of the PC calculated by FEM with (a) the dominant polarization of each modes and (b) deaf modes. (c) Transmission calculated by FEM and electrical measurements.

placement vector component for each point. In Fig. 4(b), we plot the same band diagram but with indication of whether modes may be seen as deaf or not.[17] This deaf character is based on the evaluation of the overlap of the incident S0 Lamb mode in the AlN membrane with each individual Bloch mode in the PC.[18] As can be seen, most modes are deaf between 600 and 825 MHz, except for the three bands labeled "a," "b," and "c." The inability to excite these modes in the PC is directly responsible for the transmission decrease in this frequency range. The frequency at which the band of mode "a" meets the X point of the irreducible Brillouin zone corresponds to the beginning of the measured attenuation. A transmission peak is visible in Fig. 4(c) around 700 MHz that can be identified with band "b," while band "c" lives on a flat band that yields a narrow transmission peak near 770 MHz. Above the band gap, bands "d" and "e" are the only ones that may be efficiently excited in the crystal. Band "d" is nearly flat for most wave vectors and has an in-plane transverse polarization for the other wave vectors, and thus corresponds to a small narrow peak in the transmission. Band "e" corresponds to the end of the measured attenuation.

As a conclusion, we have presented a PC fabricated in an AlN slab, with a theoretical frequency band gap extending around 800 MHz. Optical measurements realized at GHz frequencies confirm the existence of this band gap but electrical measurements reveal a wider attenuation bandwidth extending from 600 to 900 MHz, corresponding to a relative bandwidth of 40%. Theoretical investigations based on the FEM explain this phenomenon by the low transmission of Lamb waves outside of the phononic band gap that results from the existence of deaf or weakly piezoelectrically coupled Bloch modes. This work shows that, for potential applications where PCs are used for their reflector properties, considering the conversion of modes at the boundaries of a PC complements the band structure analysis and provides more insight into the behavior of the crystal.

This work was partly funded by the French Public Authorities through the NANO 2012 program. The authors would like to thank Patrick Brunet-Manquat and Sophie Verrun for their help to prepare the samples for optical measurement.

[1]M. Sigalas and E. N. Economou, Solid State Commun. **86**, 141 (1993).
[2]M. S. Kushwaha, P. Halevi, L. Dobrzynski, and B. Djafari-Rouhani, Phys. Rev. Lett. **71**, 2022 (1993).
[3]T. T. Wu, L. C. Wu, and Z. G. Huang, J. Appl. Phys. **97**, 094916 (2005).
[4]S. Benchabane, A. Khelif, J. Y. Rauch, and V. Laude, Phys. Rev. E **73**, 065601 (2006).
[5]D. M. Profunser, O. B. Wright, and O. Matsuda, Phys. Rev. Lett. **97**, 055502 (2006).
[6]C. Y. Huang, J. H. Sun, and T. T. Wu, Appl. Phys. Lett. **97**, 031913 (2010).
[7]S. Mohammadi, A. A. Eftekhar, A. Khelif, W. Hunt, and A. Adibi, Appl. Phys. Lett. **92**, 221905 (2008).
[8]N. K. Kuo, C. Zuo, and G. Piazza, Appl. Phys. Lett. **95**, 093501 (2009).
[9]M. F. Su, R. H. Olsson III, Z. C. Leseman, and I. El-Kady, Appl. Phys. Lett. **96**, 053111 (2010).
[10]Y. M. Soliman, M. F. Su, Z. C. Leseman, C. M. Reinke, I. F. El-Kady, and R. H. Olsson III, Appl. Phys. Lett. **97**, 193502 (2010).
[11]V. Yantchev and I. Katardjiev, IEEE Trans. Ultrason. Ferroelectr. Freq. Control **54**, 87 (2007).
[12]M. Gorisse, F. Domingue, G. Polo Filisan, C. Billard, I. Koné, A. Reinhardt, E. Defaÿ, and M. Aïd, Proc.-IEEE Ultrason. Symp. (in press).
[13]K. Kokkonen, M. Kaivola, S. Benchabane, A. Khélif, and V. Laude, Appl. Phys. Lett. **91**, 083517 (2007).
[14]J. V. Sánchez-Pérez, D. Caballero, R. Mártinez-Sala, C. Rubio, J. Sánchez-Dehesa, F. Meseguer, J. L. Linares, and F. Gálves, Phys. Rev. Lett. **80**, 5325 (1998).
[15]P. Vairac and B. Cretin, Opt. Commun. **132**, 19 (1996).
[16]M. Wilm, A. Reinhardt, V. Laude, R. Armati, W. Daniau, and S. Ballandras, Ultrasonics **43**, 457 (2005).
[17]F.-L. Hsiao, A. Khelif, H. Moubchir, A. Choujaa, C.-C. Chen, and V. Laude, J. Appl. Phys. **101**, 044903 (2007).
[18]T. C. Wu, T. T. Wu, and J. C. Hsu, Phys. Rev. B **79**, 104306 (2009).

Author complimentary copy. Redistribution subject to AIP license or copyright, see http://apl.aip.org/apl/copyright.jsp